

Research article

Open Access

## Physicochemical characterization of the endotoxins from *Coxiella burnetii* strain Priscilla in relation to their bioactivities

Rudolf Toman<sup>1</sup>, Patrick Garidel<sup>2</sup>, Jörg Andrä<sup>3</sup>, Katarina Slaba<sup>1</sup>, Ahmed Hussein<sup>1,5</sup>, Michel HJ Koch<sup>4</sup> and Klaus Brandenburg\*<sup>3</sup>

Address: <sup>1</sup>Institute of Virology, Slovak Academy of Sciences, Dubravská cesta 9, 84245 Bratislava, Slovak Republic, <sup>2</sup>Martin-Luther-Universität Halle, Institut für Physikalische Chemie, Mühlpforte 1, 06108 Halle, Germany, <sup>3</sup>Forschungszentrum Borstel, Div. of Biophysics, Parkallee 10, D-23845 Borstel, Germany, <sup>4</sup>European Molecular Biology Laboratory, Hamburg outstation, EMBL c/o DESY, Notkestr. 85, D-22603 Hamburg and <sup>5</sup>Present address: Dept. of Bioscience and Technology, Inst. of Graduate Studies and Research, Alexandria University, 163 Horreya Av., Chatby, 21131 Alexandria, Egypt

Email: Rudolf Toman - virutoma@savba.sk; Patrick Garidel - patrick.garidel@t-online.de; Jörg Andrä - jandrae@fz-borstel.de; Katarina Slaba - viruslab@savba.sk; Ahmed Hussein - unarc@hotmail.com; Michel HJ Koch - koch@embl-hamburg.de; Klaus Brandenburg\* - kbranden@fz-borstel.de

\* Corresponding author

Published: 12 January 2004

Received: 25 September 2003

BMC Biochemistry 2004, 5:1

Accepted: 12 January 2004

This article is available from: <http://www.biomedcentral.com/1471-2091/5/1>

© 2004 Toman et al; licensee BioMed Central Ltd. This is an Open Access article: verbatim copying and redistribution of this article are permitted in all media for any purpose, provided this notice is preserved along with the article's original URL.

### Abstract

**Background:** *Coxiella burnetii* is the etiological agent of Q fever found worldwide. The microorganism has like other Gram-negative bacteria a lipopolysaccharide (LPS, endotoxin) in its outer membrane, which is important for the pathogenicity of the bacteria. In order to understand the biological activity of LPS, a detailed physico-chemical analysis of LPS is of utmost importance.

**Results:** The lipid A moiety of LPS is tetraacylated and has longer (C-16) acyl chains than most other lipid A from enterobacterial strains. The two ester-linked 3-OH fatty acids found in the latter are lacking. The acyl chains of the *C. burnetii* endotoxins exhibit a broad melting range between 5 and 25°C for LPS and 10 and 40°C for lipid A. The lipid A moiety has a cubic inverted aggregate structure, and the inclination angle of the D-glucosamine disaccharide backbone plane of the lipid A part with respect to the membrane normal is around 40°. Furthermore, the endotoxins readily intercalate into phospholipid liposomes mediated by the lipopolysaccharide-binding protein (LBP). The endotoxin-induced tumor necrosis factor  $\alpha$  (TNF $\alpha$ ) production in human mononuclear cells is one order of magnitude lower than that found for endotoxins from enterobacterial strains, whereas the same activity as in the latter compounds is found in the clotting reaction of the *Limulus* amoebocyte lysate assay.

**Conclusions:** Despite a considerably different chemical primary structure of the *C. burnetii* lipid A in comparison with enterobacterial lipid A, the data can be well understood by applying the previously presented conformational concept of endotoxicity, a conical shape of the lipid A moiety of LPS and a sufficiently high inclination of the sugar backbone plane with respect to the membrane plane. Importantly, the role of the acyl chain fluidity in modulating endotoxicity now becomes more evident.

## Background

*Coxiella burnetii* is the etiological agent of Q fever, which belongs to the most frequent diseases of rickettsial origin in the world. The most common, acute form of Q fever is characterized as a flue-like illness or atypical pneumonia, or less frequently as granulomatous hepatitis, with a significant incidence of neurologic complications [1]. Persistent infections in humans can lead to a chronic form of Q fever, which may be associated with an often fatal endocarditis [2]. One of the main components of *C. burnetii* outer membrane is lipopolysaccharide (LPS), which plays an important role in the interaction of the microbe with the host and determines its pathogenicity and its immunogenicity [3-6]. Several papers [7-12] were devoted to the chemical characterization of the carbohydrate region of *C. burnetii* LPS. Two branched sugars virenose (6-deoxy-3-C-methyl-D-glucose) and dihydrohydroxystreptose [3-C-(hydroxymethyl)-L-lyxose], were detected mainly in terminal positions in the O-polysaccharide chain of the LPS in considerable amounts [13-15]. As these sugars have not been found in other LPS, they are important chemotaxonomic markers. We have recently shown that they might be involved in the immunobiology of Q fever [16] and presented preliminary data on the lipid A moiety of the *C. burnetii* LPS strains Henzerling and S [17]. The possible role of the LPS in the immunobiology of *C. burnetii* remains a matter of debate. In order to cast more light on this problem, we report the results of investigations on the physico-chemical behaviour of the *C. burnetii* LPS and lipid A in relation to their bioactivity, based on the established correlation between the biological activity of endotoxins and particular physico-chemical parameters [18,19]. The results are reported herein.

## Results

### Chemical composition of lipid A

Lipid A released from the parent LPS strain Priscilla on treatment with sodium acetate buffer containing SDS was shown to contain GlcN and phosphate in the molar ratio of 1:0.90. GC analysis revealed that GlcN had the D configuration. No other sugars or pyrophosphate were detected.

Fatty acids were analyzed by GC and GC-MS after mild and strong methanolyses of the lipid A followed by trimethylsilylation. Analyses revealed the presence of five different linear or branched nonhydroxy fatty acids and of eight (*R*)-configured 3-hydroxy fatty acids (Table 1). Fatty acids amounting less than 2 mol% were not considered. The major nonhydroxy fatty acids were normal hexadecanoic and 12-methyltetradecanoic acids (nC16:0 and aC15:0). The most prominent 3-hydroxy fatty acids were (*R*)-3-hydroxy-14-methylpentadecanoic and (*R*)-3-hydroxyhexadecanoic acids (3-OH-iC16:0 and 3-OH-nC16:0). GC-MS data of the analyzed samples indicated

**Table 1: Fatty acid composition of the lipid A from *C. burnetii* strain Priscilla**

Fatty acid	Amount in mol%
nC14:0	2.6
aC15:0	14.3
nC16:0	16.2
aC17:0	3.2
nC18:0	5.3
3-OH-iC14:0	4.5
3-OH-nC14:0	3.8
3-OH-iC15:0	3.5
3-OH-aC15:0	8.8
3-OH-nC15:0	2.9
3-OH-iC16:0	16.1
3-OH-nC16:0	14.8
3-OH-nC17:0	4.0

n, normal fatty acids; i, a, iso, anteiso-branched fatty acids.

that nonhydroxy fatty acids were ester-linked and hydroxylated fatty acids were amide-linked. No fatty acids were detected under conditions used for the liberation of 3-acyloxyacyl groups [20].

### Distribution of fatty acids on the D-glucosamine disaccharide analysed by MALDI mass spectrometry

The negative-ion MALDI mass spectrum of diphosphoryl lipid A gave a cluster of four ions with two main molecular ion signals at  $m/z$  1485.12 [ $M_1 - H$ ]<sup>-</sup> and 1471.53 [ $M_2 - H$ ]<sup>-</sup>. Compositions of the corresponding molecular species were established on the basis of the overall chemical composition:  $m/z$  1485.12 corresponds to two GlcNs (2 × 161.2 u), two phosphates (2 × 80 u), two C16:0 (2 × 238.5 u), and two 3-OH-C16:0 (2 × 254.5 u). The molecular species at  $m/z$  1471.53 differed from  $M_1$  by a mass difference of -14 (CH<sub>2</sub>). From the fatty acid composition given in Table 1 it can be judged that one C16:0 was substituted by a C15:0. Other cluster signals represented mass differences ± 14 (CH<sub>2</sub>), which indicated a considerable microheterogeneity of the lipid A moiety with regard to the substitution by fatty acids of different lengths. The MALDI MS data were in agreement with the negative-ion plasma desorption mass spectrum of the same lipid A sample, which also exhibited two main molecular ion signals at  $m/z$  1485 and 1471 (Caroff, M., Toman, R., unpublished results). In the lower mass range, there was a group of three peaks at  $m/z$  732.31, 748.26, and 777.48. From the known fragmentation [21] in the negative ion-mode, the first two represent Z<sub>1</sub> and Y<sub>1</sub> fragments comprising the GlcN I moiety consisting of one GlcN, one phosphate, one C16:0, and one 3-OH-C16:0 without and with the oxygen atom joining it to GlcN II (Fig. 1). The peak at  $m/z$  777.48 can be assigned to the GlcN I moiety (733 u) plus

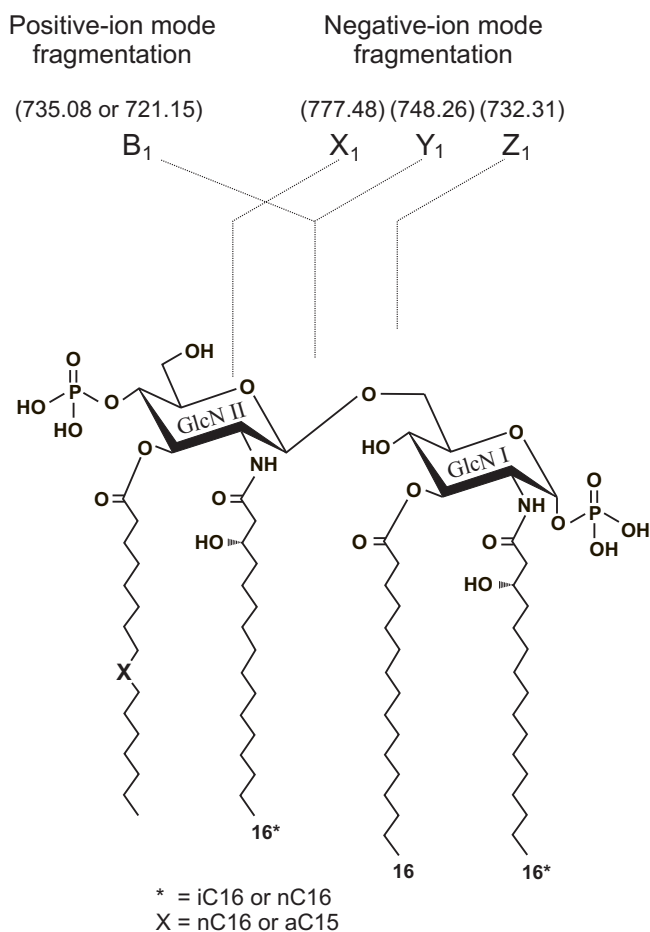


**Figure 1**  
Chemical structures of two major molecular species present in the lipid A from *C. burnetii* strain Priscilla

OHCO (45 u) from the GlcN II ring by a double cleavage of C5'-O and C1' -C2' (fragment X<sub>1</sub>).

In the positive-ion mode, MALDI MS gave one cluster of ions centered around that with  $m/z$  735.08. This peak and the other one at  $m/z$  721.15 were interpreted to correspond to the B<sub>1</sub> ions [21] containing one GlcN, one phosphate, one C16:0, one 3-OH-C16:0 and one GlcN, one phosphate, one C15:0, and one 3-OH-C16:0, respectively (Fig. 1). From this fragmentation pattern, we concluded that the signals correspond to the GlcN II part of the lipid A molecule and that C16:0 and C15:0 may alternate at the C-3' position.

#### Gel to liquid crystalline phase transition

The gel ( $\beta$ )-to-liquid crystalline ( $\alpha$ ) phase transition behaviour of the hydrocarbon chains of the *C. burnetii* LPS and lipid A was monitored by evaluation the peak posi-

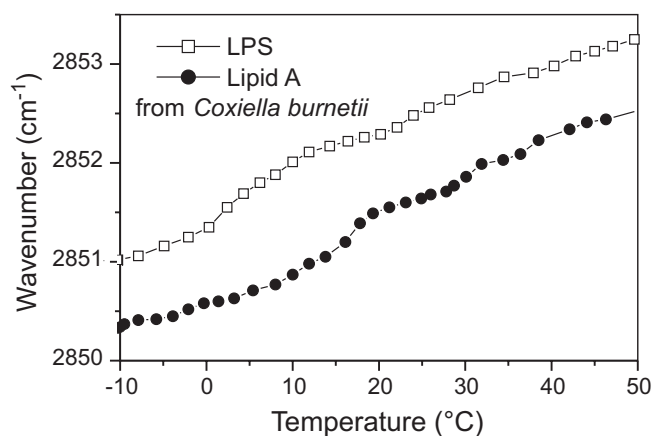


**Figure 2**  
Peak position of the symmetric stretching vibration of the methylene groups versus temperature for lipid A and LPS from *C. burnetii* strain Priscilla. In the gel phase of the hydrocarbon chains, wavenumber values are in the range 2850.0 to 2850.5  $\text{cm}^{-1}$ , in the liquid crystalline phase the respective values are 2852.5 to 2853.0  $\text{cm}^{-1}$

tion of the symmetric stretching vibrational band of the methylene groups via FTIR spectroscopy. The phase transition temperatures  $T_c$  of the samples are low as shown in Fig. 2. In the gel phase, the peak position of  $\nu_s(\text{CH}_2)$  of amphiphilic compounds is usually located between 2850.0 and 2850.5  $\text{cm}^{-1}$  and in the liquid crystalline phase between 2852.5 and 2853.0  $\text{cm}^{-1}$  [22]. This means that the transition range for the lipid A is in the temperature interval between 10 and 40–50°C, and that for the LPS in the range between – 10°C and 20°C. Note that both samples are in the liquid crystalline phase at 37°C with the LPS being significantly more fluid than lipid A.

The phase transition behaviour of lipid A was also monitored with differential scanning calorimetry (Fig. 3). In accordance with the IR measurements, a very broad transition takes place between 10 and 50°C. Two maxima at 16 and 32°C are observed in the heat capacity curve of the overall broad phase transition. These two phase transitions are also observed in the infrared experiment (Fig. 2). The phase transition enthalpies ( $\Delta H = 6 - 9$  kJ/mole), which slightly decrease upon further cycling, are considerably lower than those found for enterobacterial lipid A (20 to 30 kJ/mol [23]).

#### Molecular orientation

The angle between the diglucosamine ring plane and the membrane plane was determined by dichroic measurements using polarized IR light with oriented multilayers of the endotoxins. For this, the 0 and 90° infrared ATR

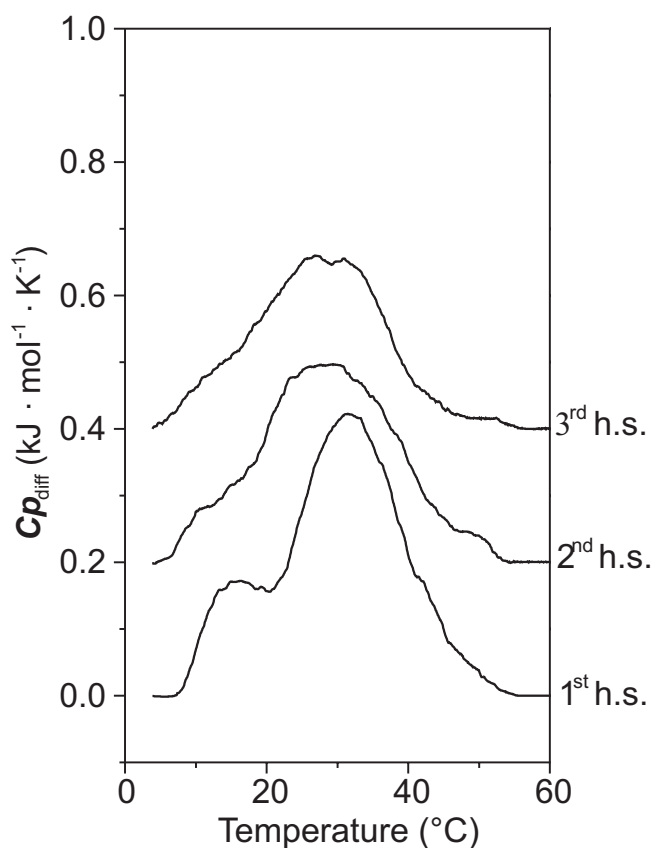


**Figure 3**

Heat capacity curves (1<sup>st</sup> to 3<sup>rd</sup> heating-scan, h.s.) of lipid A from *C. burnetii* strain Priscilla from differential scanning calorimetry. The phase transition enthalpies can be calculated from the areas of the transition and are 9, 7, and 6 kJ/mole for the respective scans.

spectra were measured (Fig. 4) and the dichroic ratios *R* of the vibrational bands around 1171 cm<sup>-1</sup> and 1040 cm<sup>-1</sup> (mean value of both bands) were calculated. Clearly, the two bands exhibit 90° polarization. The order parameter *S* was estimated from the peak position of  $\nu_s(\text{CH}_2)$ . The values of the angle  $\theta$  between the diglucosamine ring plane and the membrane plane (perpendicular to the direction of the acyl chains) calculated as described previously [18] are listed for lipid A and LPS in table 2.

The data clearly indicate that in both samples the sugar ring plane is significantly inclined with respect to the membrane plane. This inclination is, however, lower than that found for enterobacterial lipid A, for which values around 50° and higher are found, but is comparable to enterobacterial monophosphoryl (4'-phosphate) lipid A (around 35–40°) [18].

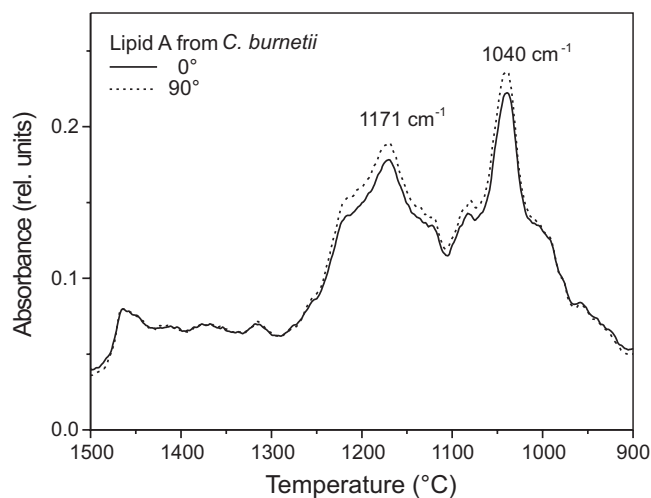


**Figure 4**

0° and 90° polarized infrared spectra of lipid A from *C. burnetii* strain Priscilla in the wavenumber range 1500 to 900 cm<sup>-1</sup>. The vibrational bands at 1171 and 1040 cm<sup>-1</sup> correspond to diglucosamine ring vibrations.

**Table 2: Dichroic ratios *R*, order parameter *S*, and inclination angle between membrane plans and diglucosamine ring plane. The *R*-values were obtained from measurements such as shown in Fig. 4.**

	Dichroic ratio <i>R</i>	Order parameter <i>S</i>	Inclination angle (°)
LPS	1.11 ± 0.03	0.61 ± 0.02	40.6 ± 2.7
Lipid A	1.10 ± 0.03	0.73 ± 0.04	38.8 ± 3.9

#### Aggregate structure

The determination of the aggregate structure of lipid A from *C. burnetii* was determined by synchrotron radiation X-ray diffraction. The X-ray pattern shown in Fig. 5 indicates the existence of a complex nonlamellar structure. However, since the relations 7.05 nm = 10.0 nm/√2, and also 7.05 nm = 12.0 nm/√3, as well as 5.43 nm = 12.0 nm/√5, and 4.33 nm = 12.0 nm/√8 hold true, at least one major substructure should have cubic symmetry.

#### Intercalation into liposomes

The intercalation of endotoxins into target cell membranes, mediated by lipopolysaccharide-binding protein (LBP), is an important step in cell activation [24,25]. The LBP-mediated intercalation of lipid A from *C. burnetii* into phospholipid liposomes was compared to that from *Salmonella minnesota* by using FRET. As illustrated in Fig. 6, addition of LBP to the liposomes in the presence of the

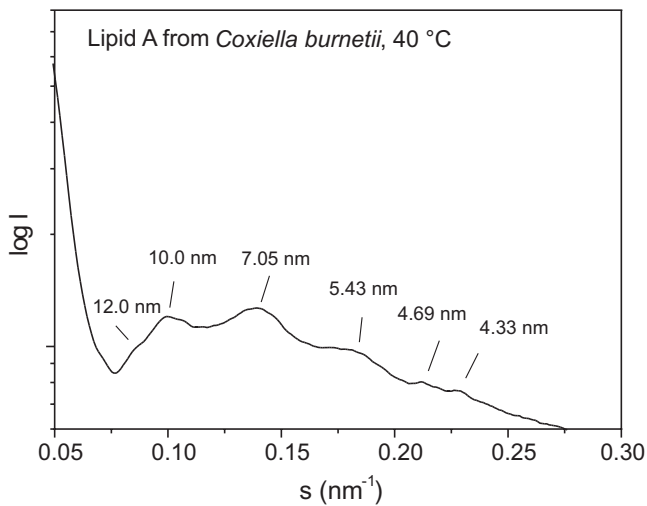


**Figure 5**  
Synchrotron radiation X-ray diffraction pattern of lipid A from *C. burnetii* strain Priscilla at 40°C and 90% water content. The logarithm of the scattering intensity log I is plotted versus the scattering vector  $s = 1/d = 2 \sin \theta / \lambda$  ( $2\theta =$  scattering angle,  $\lambda =$  wavelength = 0.15 nm)

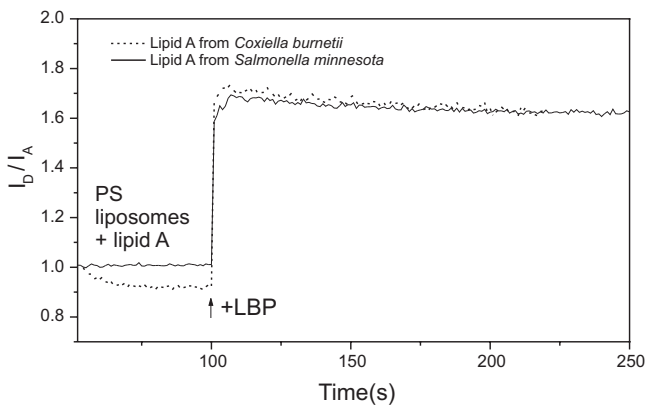


**Figure 6**  
LBP-mediated intercalation of lipid A from *C. burnetii* strain Priscilla and *S. minnesota* strain R595 into phosphatidylserine liposomes from the ratio of the donor fluorescence intensity  $I_D$  to that of the acceptor  $I_A$ . At 50 s, lipid A was added to the liposomes, and after 100 s, LBP was added.

corresponding lipid A results in a strong increase in the fluorescence signal indicating an intercalation of the two different lipid A compounds.

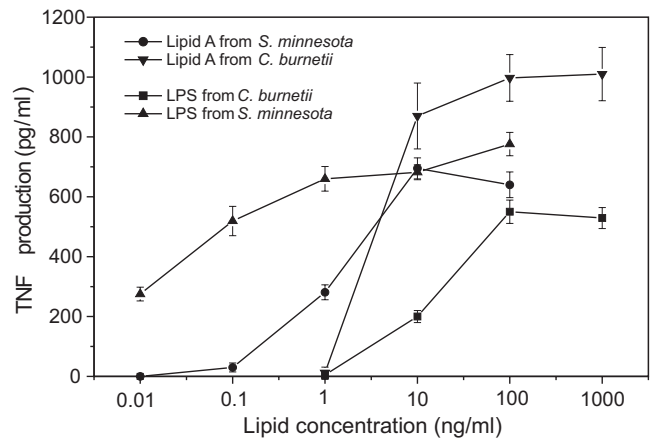


**Figure 7**  
Production of tumor-necrosis-factor  $\alpha$  (TNF $\alpha$ ) of human mononuclear cells induced by different concentrations of LPS and lipid A from *Salmonella minnesota* strain R595 and *C. burnetii* strain Priscilla. The data result from one representative experiment. The mean and standard deviation are based on the data from the determination of TNF $\alpha$  in duplicate at two different dilutions. A repetition of the experiments yielded the same dependences except for the absolute amount of TNF $\alpha$ -production which may vary significantly between different donors.

**Biological activity**

The cytokine-inducing capacity of both *C. burnetii* LPS and lipid A was tested and compared to that of LPS and lipid A from *Salmonella minnesota* strain Re 595 by stimulating human mononuclear cells (MNC). A representative result is shown in Fig. 7 indicating the highest activity for the Re LPS and one to two order of magnitude lower activity for its lipid A. In contrast, the *C. burnetii* endotoxins exhibit significantly lower activity that disappears already at the endotoxin concentration of 1 ng/ml. Interestingly, in sharp contrast to the behaviour of the *Salmonella* endotoxins, for the *Coxiella* endotoxins lipid A exhibits stronger activity than the parent LPS.

Further, the ability to induce the coagulation cascade in the LAL test was examined. A high activity down to a concentration of 10 pg/ml, independently on the origin of the endotoxins used, was found (data not shown). Thus, in contrast to the cytokine induction there is no significant difference in the induction of coagulation between the LPS and lipid A used in this study. The remarkable differences in both chemical composition and structure of the endotoxins thus apparently do not play a role in this test system.

## Discussion

In the first step of these studies we established basic structural features of the lipid A from *C. burnetii* strain Priscilla. The chemical investigations revealed that despite a considerable microheterogeneity the two major molecular species depicted in Fig. 1 are the major components. They share the classical backbone of diphosphorylated D-GlcN disaccharide, in which both GlcN I and GlcN II carry amide-linked 3-OH-iC16:0 or 3-OH-nC16:0. One of the species has ester-linked nC16:0 at both GlcNs while the other one has ester-linked aC15:0 instead of nC16:0 in GlcN II. Other less abundant molecular species are closely related to them and differ one from another only by mass difference of  $\pm 14$  (CH<sub>2</sub>) depending on the fatty acid bound.

In a previous paper [26], reporting on the fatty acid compositions of the LPS isolated from *C. burnetii* strain Nine Mile in virulent phase I and low virulent phase II, the authors have identified more than 50 different 3-acyloxyacyl residues to be involved in amide linkages. This together with the other fatty acids found suggested an enormous heterogeneity of the lipid A component in both LPS. In contrast, our results have shown that both composition and structure of the major molecular species of the investigated lipid A are quite simple as illustrated in Fig. 1. In our preliminary studies, similar structural features have been found for lipid A of the LPS from *C. burnetii* strains Henzerling and S [17], and most recently, for lipid A from the abovementioned strain Nine Mile in virulent phase I and low virulent phase II [27]. The data indicate that lipid A in various *C. burnetii* strains may represent a highly conserved region of their LPS. Thus, the chemical structure of the *C. burnetii* lipid A differs considerably from those of typical enterobacterial lipid A with high endotoxicity [28].

Distinct structural features of the lipid A could be the cause for its reduced endotoxic potency reported in this work and elsewhere [3,8], leading to unique physicochemical properties (see below) in comparison with the enterobacterial lipid A.

We have found previously that a prerequisite for the cytokine-inducing activity of a lipid A-like compound is the existence of a non-lamellar cubic aggregate structure of the lipid A moiety of LPS, which corresponds to a strictly conical shape of the single molecules [19]. Furthermore, a high inclination angle of more than 45° was observed for all biologically highly active compounds, whereas samples with medium inclination angle and moderate conical shape such as monophosphoryl lipid A were much less active [18]. Compounds with low or no inclination and with cylindrical shape such as pentaacyl and tetraacyl lipid A from *Escherichia coli* mutants were more or less

inactive, but could act antagonistically against the action of LPS. The endotoxins of *C. burnetii* fulfill the main criterion of endotoxicity, the cubic aggregate structure (Fig. 5). However, the inclination angle is much less than that found for enterobacterial hexaacylated samples (Table 2), and would correspond in the light of our concept to lipid A with significantly reduced activity. This is impressively confirmed by the results of the TNF $\alpha$ -inducing capacity in mononuclear cells (Fig. 7). In this context, it has to be noted that agonistically inactive tetraacylated lipid A (synthetic '406') with C14 chains has a much lower inclination angle, 10 to 20° [18]. The reason for this discrepancy is unclear. It has to be considered, however, that the DSC data indicate drastic differences of the enthalpy change  $\Delta H_c$  for lipid A from *Coxiella* (6–9 kJ/mole) as compared to hexaacyl lipid A from enterobacterial strains (20 to 30 kJ/mole [23]). On the basis of the number of CH<sub>2</sub> groups, the  $\Delta H_c$  for the two lipid A should be approximately the same under the prerequisite of identical packing density. This means that the packing density of the *Coxiella* lipid A must be considerably smaller. Furthermore, DSC as well as FTIR data (Figs. 2,3) are indicative of two phase transitions which could correspond to two subspecies. The various non-stoichiometric substituents may be responsible for these observations, which subsequently may lead to the observed inclination.

We have reported earlier [29,30] that the lipid A acyl chain fluidity is not a basic determinant of endotoxic activity, but may modulate it. Thus, when a lipid A and various LPS chemotypes with different lengths of sugar residues and of the same enterobacterial origin are compared, the highest activity is found for an Re LPS with a T<sub>c</sub> lying around 30°C corresponding to the highest acyl chain mobility at 37°C. For other rough mutant LPS Rd to Ra, the bioactivity slightly decreases, which seems to be correlated with an increase of T<sub>c</sub> up to 36°C corresponding to a decrease of the acyl chain mobility at 37°C [30]. The largest decrease of bioactivity is found for lipid A, which can be correlated with a drastic increase of T<sub>c</sub> up to 45°C, corresponding to gel-like hydrocarbon chains at 37°C. Thus, the remarkable differences in bioactivity of one to two orders of magnitude, observed for enterobacterial lipid A and LPS (Fig. 7), could be due to the high difference in the acyl chain mobility at 37°C.

For the *C. burnetii* endotoxins, these considerations do not hold true. It can be concluded from the data of the phase transition measurements (Fig. 2,3) that both compounds are in the liquid crystalline phase at 37°C, although the acyl chains of LPS are still more mobile than that of lipid A. However, the DSC data show (Fig. 3) that most of the lipid A acyl chains are molten at 37°C. Thus, these data have verified experimentally for the first time our assumption that the acyl chain mobility is responsible for the

large differences in biological activity between the enterobacterial LPS and lipid A. As shown in Fig. 7, the *C. burnetii* lipid A seems to be even more active than the parent LPS. These data confirm the fact that lipid A is the 'endotoxic principle' of LPS, and indicate that it is possible to discriminate between the effect of molecular conformation (shape) and acyl chain mobility.

In the *Limulus* test, identical activation by *Coxiella* and *Salmonella* LPS and lipid A were found. For an understanding, the structural requirements of the activation of the clotting cascade must be considered. By using different synthetic lipid A and part structures, Takada et al [31] have shown that the monophosphoryl 4'-phosphate lipid A has the same activity as bisphosphoryl lipid A, whereas the monophosphoryl 1-phosphate lipid A has strongly reduced activity. We have found that the interaction of LPS and lipid A with hemoglobin [32] or albumin [33] led to a strong or slight increase, respectively, of the cytokine production in mononuclear cells, but was not correlated with the results in the *Limulus* test, which exhibited somehow non-systematic variations. The binding of high-density lipoprotein (HDL) to the endotoxins, however, led to a clear, concentration-dependent decrease of the immunostimulatory activity in the human system as well as the *Limulus* activity [34]. Additionally it was found that the binding epitope of HDL within the lipid A backbone is essentially the diglucosamine headgroup inclusive the 4'-phosphate [34]. From these data the results presented here become intelligible, the 4'-phosphate diglucosamine backbone is the same for *Coxiella* and *Salmonella* lipid A, and therefore identical reactivities are observed. From these data it becomes also clear that the *Limulus* test is not a measure of toxicity of endotoxin preparations.

Although a complete interpretation of a correlation between physico-chemical parameters and bioactivity is presently not possible, there is a wealth of experimental evidence that the molecular conformation of the lipid A moiety of an LPS plays a role after intercalation into target cell membranes such as those of mononuclear cells. It has been shown previously that the intercalation is mediated by LBP (see Fig. 6) [24,25], but one may assume that also mCD14 is able to intercalate LPS after binding. In the membrane, an LPS with conically-shaped lipid A is able to induce sterical stress at the site of signalling proteins such as the Toll-like receptor 4 [35] or the K<sup>+</sup>-channel MaxiK [36] leading to transmembrane signalling.

The influence of the acyl chain mobility may be displayed in the way that the binding of LPS having more fluid acyl chains to proteins such as LBP and/or CD14 is enhanced, and in particular that the intercalation into the target cell membranes is facilitated.

## Materials and methods

### Cultivation and purification of *C. burnetii* cells

*C. burnetii* strain Priscilla (PR) was from the strain collection of the WHO Collaborating Centre for Rickettsial Reference and Research at the Institute of Virology, Slovak Academy of Sciences, Bratislava, Slovak Republic. PR was propagated in embryonated hen eggs. After cultivation, the PR cells were purified by centrifugation and extraction with ether as described earlier [11].

### Isolation of LPS and lipid A moiety

The PR cells were treated first with RNase (EC 3.1.27.5) and DNase I (EC 3.1.21.1), both from bovine pancreas (Roche, Mannheim, Germany), then with trypsin (EC 3.4.21.4, from bovine pancreas, Serva, Germany), and finally with proteinase K (EC 3.4.21.14, from Tritirachium album, Sigma, USA). The cells were extracted further with chloroform-methanol (2:1, v/v) at 20 °C for 4 h to remove phospholipids. The extraction was repeated with the fresh solvent mixture for 2 h. The crude LPS was isolated from the cells by the hot phenol/water method as described [11] and purified further by ultracentrifugation (120,000 · g) at 5 °C for 4 h until sodium dodecyl sulphate-polyacrylamide gel electrophoresis (SDS-PAGE), TLC, and UV spectroscopy showed no detectable contaminants. Lipid A was prepared from the LPS by hydrolysis with 20 mM sodium acetate/acetic acid buffer (pH 4.5) containing 1% of SDS at 100 °C for 1 h [37]. A sample of lipid A was hydrolyzed with 4 M HCl at 100 °C for 4 h.

### Preparation of lipid A sample

Lipid A samples were usually prepared as aqueous dispersions at high buffer content, i.e., above 80 % using 20 mM HEPES (pH 7). For this, the lipids were suspended directly in buffer, sonicated and temperature-cycled several times between 5 and 70 °C and then stored at 4 °C for at least 12 h before measurement.

### Analytical methods and instruments

SDS-PAGE was performed in slabs containing 12.5% of polyacrylamide and the gels were silver-stained for LPS as described [38]. TLC was accomplished on precoated Silica Gel 60 plates (Merck, Germany) with (v/v) 30/15/4.5/0.5 *n*-propanol-water-chloroform-1 M ammonium hydroxide and 4.5/3.5 isobutyric acid-1 M ammonium hydroxide solvent mixtures. Spots were visualized by charring after spraying with 10% sulphuric acid in ethanol. 3-deoxy-D-manno-2-octulosonic acid (Kdo), protein, phosphate, and hexosamine contents were determined as reported [11]. Estimation of the absolute configuration of glucosamine (GlcN) in lipids A was established as given elsewhere [39,40]. Total fatty acids were analyzed by gas chromatography (GC) and GC-mass spectrometry (GC-MS) after hydrolysis of lipid A with 4 M HCl in dry MeOH at 100 °C for 16 h and trimethylsilylation. Ester-linked fatty acids

were determined after their release with 2 M HCl in MeOH at 60°C for 2 h. The stereochemistry of 3-hydroxy fatty acids was established as described [20].

#### GC and GC-MS

GC was performed with a Shimadzu model 17A chromatograph equipped with flame-ionization detector using helium as the carrier gas. Alditol acetates of amino sugars were analyzed on an HP-5 column (25 m × 0.32 mm, Hewlett-Packard, USA) at 160 (3 min) increasing to 245°C at 3°C.min<sup>-1</sup>. Fatty acids were separated on a DB-1 column (60 m × 0.25 mm, Fison, UK) at 180 (2 min) increasing to 280°C at 4°C.min<sup>-1</sup> with a final 30 min hold. GC-MS was performed with a Shimadzu GCMS-QP5000 mass spectrometer with helium as the carrier gas. Electron impact mass spectra were recorded at 70 eV and an interface temperature of 300°C. GC-MS was run with the columns and temperature programs already described.

#### MALDI-TOF-MS

Matrix-assisted laser desorption/ionization-time-of-flight mass spectrometry (MALDI-TOF-MS) of lipid A was performed with a KOMPACT MALDI IV (Kratos Analytical, Japan) in the linear TOF configuration at an acceleration voltage of 20 kV. 2,4,6-Trihydroxyacetophenone (Aldrich, Taufkirchen, Germany) was used as the matrix. Analyte ions were desorbed from the matrix with pulses from a 326 nm nitrogen laser. Each spectrum represents an average of 60 pulses. Lipid A samples in the amount of 0.25–0.5 µg were used.

#### FTIR spectroscopy

The infrared spectroscopic measurements were performed on a IFS-55 spectrometer (Bruker, Karlsruhe, Germany). The lipid samples were placed in a CaF<sub>2</sub> cuvette with a 12.5 µm teflon spacer. Temperature-scans were performed automatically between 10 and 70°C with a heating-rate of 0.6°C.min<sup>-1</sup>. Every 3°C, 50 interferograms were accumulated, apodized, Fourier transformed, and converted to absorbance spectra. For strong absorption bands, the band parameters (peak position, band width, and intensity) were evaluated from the original spectra, if necessary after subtraction of the strong water bands.

#### Attenuated total reflectance (ATR) with polarized IR light

The lipids were prepared as oriented thin multilayers as described previously [18] by spreading a 1 mM lipid suspension – which was temperature-cycled between 5 and 70°C several times prior to spreading – in Hepes buffer on a ZnSe ATR crystal and evaporating the excess water by slow periodic movement under a nitrogen stream at room temperature. The lipid sample was placed in a closed cuvette, and the air above the sample was saturated with water vapour to maintain full hydration. Infrared ATR

polarized spectra at 0 and 90° were recorded using a mercury-cadmium-telluride (MCT) detector with a scan number of 1000 at a resolution of 2 cm<sup>-1</sup>. The measurements were performed at 28°C, the intrinsic instrument temperature.

Dichroic ratios *R* for particular vibrational bands from the diglucosamine backbone were evaluated at 1170 and 1045 cm<sup>-1</sup>. The angle  $\theta$  represents the angle between the diglucosamine diphosphorylated backbone and the direction of the hydrocarbon chains, and can be calculated from the measured *R*, if an approximate value of the order parameter *S* is known. As a first approximation, the *S*-value calculated according to the relationship between *S*,  $\theta$ , and *R*, based on the peak position  $x_s$  of the symmetric stretching vibration  $\nu_s(\text{CH}_2)$  can be used, where *S* is calculated according to  $S = -941.8 + 0.7217 \cdot x_s - 7.823 \cdot 10^{-5} \cdot x_s^2 - 2.068 \cdot 10^{-8} \cdot x_s^3$ . It should be noted that *S* defined in this way should be similar, but not identical to the order parameter used in NMR spectroscopy (*S* = 1 for perfectly aligned and 0 for isotropic acyl chains).

Since the hydrocarbon chains of the lipid multilayer are distributed homogeneously around the normal to the ATR plate ('partial axial distribution'), a tilt of the backbone with respect to the direction of the acyl chains leads to a broader orientational distribution of the backbone, which would correspond to a lower *S*-value. This implies that the acyl chains are more isotropically distributed and that the estimate of *S* is an upper limit.

The water content of the samples on the ATR crystal, which is important for an exact calculation of the *z*-component of the electric field,  $E_z$ , was estimated from the ratio between the peak intensities of the main OH-stretch around 3400 cm<sup>-1</sup> and the antisymmetric stretch of the methylene groups around 2920 cm<sup>-1</sup>. Since this ratio depends on the chemical composition of the particular lipid/protein sample at a given water content, each sample was calibrated by recording IR spectra in transmission at various water contents and determining the corresponding peak ratios.

#### Differential scanning calorimetry

Differential scanning calorimetry (DSC) measurements were performed with a MicroCal VP scanning calorimeter (MicroCal, Inc., Northampton, MA, USA). The heating and cooling rate was 1°C/min. Heating and cooling curves were measured in the temperature interval from 10 to 100°C. The phase transition enthalpy is obtained by integration of the heat capacity curve as described previously [41]. Usually, three consecutive heating and cooling scans were measured. The lipid dispersion is prepared according to recently described protocols at a

concentration of approximately 1 mg/ml in phosphate buffer at pH 6.8 [42].

### X-ray diffraction

X-ray diffraction measurements were performed at the European Molecular Biology Laboratory (EMBL) outstation at the Hamburg synchrotron radiation facility HASYLAB using the double-focusing monochromator-mirror camera X33 [43]. Diffraction patterns in the range of the scattering vector  $0.07 < s < 1 \text{ nm}^{-1}$  ( $s = 2 \sin \theta / \lambda$ ,  $2\theta$  scattering angle and  $\lambda$  the wavelength = 0.15 nm) were recorded at 40°C with exposure times of 2 or 3 min using a linear detector with delay line readout [44]. The s-axis was calibrated with tripalmitate, which has a periodicity of 4.06 nm at room temperature. Details of the data acquisition and evaluation system can be found elsewhere [45]. The diffraction patterns were evaluated as described previously [46] assigning the spacing ratios of the main scattering maxima to defined three-dimensional structures. The lamellar and cubic structures are most relevant here. They are characterized by the following features:

(1) Lamellar: The reflections are grouped in equidistant ratios, i.e., 1, 1/2, 1/3, 1/4, etc. of the lamellar repeat distance  $d_l$

(2) Cubic: The different space groups of these non-lamellar three-dimensional structures differ in the ratio of their spacing. The relation between reciprocal spacing  $s_{hkl} = 1/d_{hkl}$  and lattice constant  $a$  is

$$s_{hkl} = [(h^2 + k^2 + l^2) / a^2]^{1/2}$$

(hkl = Miller indices of the corresponding set of plane).

### Fluorescence resonance energy transfer spectroscopy (FRET)

The FRET assay was performed as described earlier [24,25]. Briefly, phospholipid liposomes from phosphatidylserine (PS) or from a phospholipid mixture corresponding to the composition of the macrophage membrane [47] were doubly labelled with the fluorescent dyes N-(7-nitrobenz-2-oxa-1,3-diazol-4-yl)-phosphatidylethanolamine (NBD-PE) and N-(lissamine rhodamine B sulfonyl)-phosphatidylethanolamine (Rh-PE) (Molecular Probes, Eugene, OR, USA). Intercalation of unlabeled molecules into the doubly labelled liposomes leads to probe dilution and with that to a lower FRET efficiency: the emission intensity of the donor increases and that of the acceptor decreases.

In all experiments, doubly labelled phospholipid liposomes were prepared and after 50 and 100 s, respectively, lipid A and LBP were added subsequently, each at a final concentration of 0.01 mM, and the NBD donor fluores-

cence intensity  $I_D$  at 531 nm and acceptor intensity  $I_A$  at 593 nm were monitored for at least 300 s. As sensitive signal of a membrane intercalation, the ratio  $I_D/I_A$  was plotted versus time.

### Stimulation of human mononuclear cells

For examination of the cytokine-inducing capacity of the LPS and its lipid A, human mononuclear cells (MNC) were stimulated with the latter compound and the TNF $\alpha$  production of the cells was determined in the supernatant.

MNC were isolated from heparinized (20 IE · mL<sup>-1</sup>) blood taken from healthy donors and processed directly by mixing with an equal volume of Hank's balanced solution and centrifugation on a Ficoll density gradient for 40 min (21°C, 500 g). The layer of HMNC was collected and washed twice in Hank's medium and once in RPMI 1640 containing 4% human serum, 2 mM L-glutamine, 100 U · mL<sup>-1</sup> penicillin, and 100  $\mu$ g · mL<sup>-1</sup> streptomycin. The cells were resuspended in medium and their number was equilibrated at  $5 \times 10^6$  cells · mL<sup>-1</sup>. For stimulation, 200  $\mu$ L/well MNC ( $5 \times 10^6$  cells · mL<sup>-1</sup>) were transferred into 96-well culture plates. The stimuli were serially diluted in medium and added to the cultures at 20  $\mu$ L per well. The cultures were incubated for 4 h at 37°C under 5 % CO<sub>2</sub>. Supernatants were collected after centrifugation of the culture plates for 10 min at 400 g and stored at -20°C until determination of the cytokine content. Determination of TNF $\alpha$  in the cell supernatant was performed in a sandwich-ELISA as described elsewhere [48]. Briefly, 96-well microtiter plates (Greiner, Solingen, Germany) were coated overnight at room temperature with a monoclonal (mouse) anti-human TNF $\alpha$  antibody (clone 16 from Intex AG, Switzerland) followed by three washings with water. One hundred microliter samples of culture supernatants were dispensed into the wells and incubated with HRP-conjugated rabbit anti-human TNF $\alpha$  antibody (Intex) for 16–24 h at 4°C. After washing, the color reaction was started by addition of tetramethylbenzidine/H<sub>2</sub>O<sub>2</sub> and stopped by the addition of 1 M sulfuric acid. Serial dilutions of human recombinant TNF $\alpha$  (Intex) provided a standard curve. Plates were read at 450 nm with an ELISA photometer. Quantification of TNF $\alpha$  was determined with detection ranges of 0–500 pg/ml. TNF $\alpha$  content was determined for each condition and the data given are average values  $\pm$  SD from the TNF $\alpha$  determination in duplicate at two different dilutions. The data shown here represent one of at least three independent experiments.

### Determination of the endotoxin activity by the chromogenic Limulus test

Endotoxin activity of the LPS and its lipid A was determined at the concentrations between 10  $\mu$ g · mL<sup>-1</sup> and 10 pg · mL<sup>-1</sup> with the *Limulus* amoebocyte lysate (LAL) test kit

[49] from LAL Coamatic Chromo-LAL K (Chromogenix, Haemochrom). The standard endotoxin used in this test was from *Escherichia coli* (O55:B5), and 10 EU · ml<sup>-1</sup> corresponds to 1 ng · ml<sup>-1</sup>. In this assay, saturation occurs at 125 endotoxin units EU · ml<sup>-1</sup>, and the resolution limit is ≤ 0.1 EU · ml<sup>-1</sup> (maximum value for ultra pure water from embryo-transfer, Sigma).

### Authors' contribution

RT supervised cultivation and isolation procedures, GC- and MALDI-TOF-MS analyses, and wrote the chemical part of the manuscript, PG performed the DSC, JA the IR-spectroscopic measurements, KS accomplished cultivation and purification of the *C. burnetii* strain Priscilla cells, AH isolated the LPS and lipid A, and run GC- and MALDI-TOF-MS analyses, MHJK the synchrotron radiation X-ray diffraction measurements, and KB supervised the FRET- and biological experiments and drafted the manuscript.

### Acknowledgements

We are indebted to G. von Busse, U. Diemer, and K. Stephan for technical assistance in the IR spectroscopic, LAL and TNF $\alpha$  measurements, respectively. B. Fölting is acknowledged for excellent technical assistance in the DSC experiments. This work was supported in part by grant No. 2/3021/23 of the Scientific Grant Agency of the Ministry of Education of the Slovak Republic and Slovak Academy of Sciences. Furthermore, this work has been carried out with financial support from the Commission of the European Communities, specific RTD programme "Quality of Life and Management of Living Resources", QLK-CT-2002-01001, 'Antimicrobial endotoxin neutralizing peptides to combat infectious diseases'.

### References

- Marrie TJ: **Acute Q fever.** In *Q Fever. The Disease Volume I.* Edited by: Marrie TJ. Boca Raton: CRC Press; 1990:125-160.
- Raoult D, Raza A, Marrie TJ: **Q fever endocarditis and other forms of chronic Q fever.** In *Q Fever. The Disease* Edited by: Marrie TJ. Boca Raton: CRC Press; 1990:179-199.
- Williams JC, Waag DM: **Antigens, virulence factors, and biological response modifiers of Coxiella burnetii: Strategies for vaccine development.** In *Q Fever, The Biology of Coxiella burnetii* Edited by: Williams JC, Thompson HA. Boca Raton: CRC Press; 1991:175-222.
- Gajdošová E, Kováčová E, Toman R, Škultéty L', Lukáčová M, Kazár J: **Immunogenicity of Coxiella burnetii whole cells and their outer membrane components.** *Acta Virol* 1994, **38**:339-344.
- Dellacasagrande J, Ghigo E, Machergui-El Hammami S, Toman R, Raoult D, Capo C, Mege JL:  **$\alpha_v\beta_3$  Integrin and bacterial lipopolysaccharide are involved in Coxiella burnetii-stimulated production of tumor necrosis factor by human monocytes.** *Infect Immun* 2000, **68**:5673-5678.
- Hussein A, Kováčová E, Toman R: **Isolation and evaluation of Coxiella burnetii O-polysaccharide antigen as an immunodiagnostic reagent.** *Acta Virol* 2001, **45**:173-180.
- Schramek Š, Mayer H: **Different sugar compositions of lipopolysaccharides isolated from phase I and pure phase II cells of Coxiella burnetii.** *Infect Immun* 1982, **38**:53-57.
- Amano K, Williams JC, Missler SR, Reinhold VN: **Structure and biological relationships of Coxiella burnetii lipopolysaccharides.** *J Biol Chem* 1987, **262**:4740-4747.
- Toman R, Kazár J: **Evidence for the structural heterogeneity of the polysaccharide component of Coxiella burnetii strain Nine Mile lipopolysaccharide.** *Acta Virol* 1991, **35**:531-537.
- Toman R, Škultéty L': **Structural study on a lipopolysaccharide from Coxiella burnetii strain Nine Mile in a virulent phase II.** *Carbohydr Res* 1996, **283**:175-185.
- Škultéty L', Toman R, Pätoprstý V: **A comparative study of lipopolysaccharides from two Coxiella burnetii strains considered to be associated with acute and chronic Q fever.** *Carbohydr Polymers* 1998, **35**:189-194.
- Ftáček P, Škultéty L', Toman R: **Phase variation of Coxiella burnetii strain Priscilla: Influence of this phenomenon on biochemical features of its lipopolysaccharide.** *J Endotoxin Res* 2000, **6**:369-376.
- Schramek Š, Radziejewska-Lebrecht J, Mayer H: **3-C-Branched aldoses in lipopolysaccharides of phase I Coxiella burnetii and their role as immunodominant factors.** *Eur J Biochem* 1985, **148**:455-461.
- Toman R: **Basic structural features of a lipopolysaccharide from the Coxiella burnetii strain Nine Mile in the virulent phase I.** *Acta Virol* 1991, **35**:224.
- Toman R, Škultéty L', Ftáček P, Hricovini M: **NMR study of virenose and dihydrohydroxystreptose isolated from Coxiella burnetii phase I lipopolysaccharide.** *Carbohydr Res* 1998, **306**:291-296.
- Slabá K, Hussein A, Palkovič P, Horváth V, Toman R: **Studies on the immunological role of virenose and dihydrohydroxystreptose present in the Coxiella burnetii phase I lipopolysaccharide.** *Ann NY Acad Sci* 2003, **990**:505-509.
- Toman R, Hussein A, Palkovič P, Ftáček P: **Structural properties of lipopolysaccharides from Coxiella burnetii strains Henzlerling and S.** *Ann NY Acad Sci* 2003, **990**:563-567.
- Seydel U, Oikawa M, Fukase K, Kusumoto S, Brandenburg K: **Intrinsic conformation of lipid A is responsible for agonistic and antagonistic activity.** *Eur J Biochem* 2000, **267**:3032-3039.
- Schromm A, Brandenburg K, Loppnow H, Moran AP, Koch MHJ, Rietschel Eth, Seydel U: **Biological activities of lipopolysaccharides are determined by the shape of their lipid A portion.** *Eur J Biochem* 2000, **267**:2008-2013.
- Wollenweber HW, Rietschel ET: **Analysis of lipopolysaccharide (lipid A) fatty acids.** *J Microbiol Methods* 1990, **11**:195-211.
- Costello CE, Vath JE: **Tandem mass spectrometry of glycolipids.** *Methods Enzymol* 1990, **193**:738-768.
- Mantsch HH, McElhaney RN: **Phospholipid phase transitions in model and biological membranes as studied by infrared spectroscopy.** *Chem Phys Lipids* 1991, **57**:213-226.
- Brandenburg K, Seydel U: **Physical aspects of structure and function of membranes made from lipopolysaccharides and free lipid A.** *Biochim Biophys Acta* 1984, **775**:225-238.
- Schromm AB, Brandenburg K, Rietschel ETH, Flad H-D, Carroll SF, Seydel U: **Lipopolysaccharide-binding protein mediates CD14-independent intercalation of lipopolysaccharide into phospholipid membranes.** *FEBS Letters* 1996, **399**:267-271.
- Gutsmann T, Schromm AB, Koch MHJ, Kusumoto S, Fukase K, Oikawa M, Seydel U, Brandenburg K: **Lipopolysaccharide-binding protein-mediated interaction of lipid A from different origin with phospholipid membranes.** *Phys Chem Chem Phys* 2000, **2**:4521-4528.
- Wollenweber HW, Schramek Š, Moll H, Rietschel ET: **Nature and linkage of fatty acids present in lipopolysaccharides of phase I and phase II Coxiella burnetii.** *Arch Microbiol* 1985, **142**:6-11.
- Hussein A, Caroff M, Toman R: **Lipid A of Coxiella burnetii strain Nine Mile in virulent phase I and low-virulent phase II: chemical composition and structure.** *Book of Abstracts, 12th European Carbohydrate Symposium, Grenoble, France* :68. July 6-11 2003
- Alexander C, Rietschel ET: **Bacterial lipopolysaccharides and innate immunity.** *J Endotoxin Res* 2001, **7**:167-202.
- Seydel U, Wiese A, Schromm AB, Brandenburg K: **Biophysical view on the function and activity of endotoxins.** In *Endotoxin in Health and Disease* Edited by: Brade H, Opal SM, Vogel SN, Morrison DC. New York and Basel: Marcel Dekker; 1999:195-219.
- Seydel U, Labischinski H, Kastowsky M, Brandenburg K: **Phase behaviour, supramolecular structure, and molecular conformation of lipopolysaccharide.** *Immunobiol* 1993, **187**:191-211.
- Takada H, Kotani S, Tanaka S, Ogawa T, Takahashi I, Tsujimoto M, Komuro T, Shiba T, Kusumoto S, Kusunose N, Hasegawa A, Kiso M: **Structural requirements of lipid A species in activation of clotting enzymes from the horseshoe crab, and the human complement cascade.** *Eur J Biochem* 1988, **175**:573-580.
- Jürgens G, Müller M, Koch MHJ, Brandenburg K: **Interaction of hemoglobin with enterobacterial lipopolysaccharide and lipid A.** *Eur J Biochem* 2001, **268**:4233-4242.

33. Jürgens G, Müller M, Garidel P, Koch MHJ, Nakakubo H, Blume A, Brandenburg K: **Investigation into the interaction of recombinant human serum albumin with Re-lipoplysaccharide and lipid A.** *J Endotoxin Res* 2002, **8**:115-126.
34. Brandenburg K, Jürgens G, Andrä J, Lindner B, Koch MHJ, Blume A, Garidel P: **Biophysical characterization of the interaction of high-density lipoprotein (HDL) with endotoxins.** *Eur J Biochem* 2002, **269**:5972-5981.
35. Chow JC, Young DW, Golenbock DT, Christ WJ, Gusovsky F: **Toll-like receptor-4 mediates lipopolysaccharide-induced signal transduction.** *J Biol Chem* 1999, **274**:10689-10692.
36. Blunck R, Scheel O, Müller M, Brandenburg K, Seitzer U, Seydel U: **New insights into endotoxin-induced activation of macrophages: Involvement of a K<sup>+</sup> channel in transmembrane signaling.** *J Immunol* 2001, **166**:1009-1015.
37. Caroff M, Tacke A, Szabo L: **Detergent-accelerated hydrolysis of bacterial endotoxins and determination of the anomeric configuration of the glycosyl phosphate present in the "isolated lipid A" fragment of the *Bordetella pertussis* endotoxin.** *Carbohydr Res* 1988, **175**:273-282.
38. Škultéty L, Toman R: **Improved procedure for the drying and storage of polyacrylamide slab gels.** *J Chromatogr* 1992, **582**:249-252.
39. Gerwig GJ, Kamerling JP, Vliegthart JF: **Determination of the absolute configuration of monosaccharides in complex carbohydrates by capillary G.L.C.** *Carbohydr Res* 1979, **77**:10-17.
40. Aussel L, Brisson JR, Perry MB, Caroff M: **Structure of the lipid A of *Bordetella hinzii* ATCC 51730.** *Rapid Commun Mass Spectrom* 2000, **14**:595-599.
41. Blume A, Garidel P: **Lipid model membranes and biomembranes.**, In *From Macromolecules to Man* Edited by: Kemp RB. Amsterdam, Elsevier; 1999:109-173.
42. Garidel P, Blume A: **The interaction of alkaline earth cations with the negatively charged phospholipid 1,2-dimyristoyl-sn-glycero-3-phosphoglycerol: a differential scanning and isothermal titration calorimetric study.** *Langmuir* 1999, **15**:5526-5534.
43. Koch MHJ, Bordas J: **X-ray diffraction and scattering on disordered systems using synchrotron radiation.** *Nucl Instrum Methods* 1983, **208**:461-469.
44. Gabriel A: **Positive-sensitive X-ray detector.** *Rev Sci Instrum* 1977, **48**:1303-1305.
45. Boulin C, Kempf R, Koch MHJ, McLaughlin S: **Data appraisal, evaluation and display for synchrotron radiation experiments: Hardware and software.** *Nucl Instr Meth* 1986, **A249**:399-407.
46. Brandenburg K, Funari SS, Koch MHJ, Seydel U: **Investigation into the acyl chain packing of endotoxins and phospholipids under near physiological conditions by WAXS and FTIR spectroscopy.** *J Struct Biol* 1999, **128**:175-186.
47. Kröner EE, Peskar BA, Fischer H, Ferber E: **Control of arachidonic acid accumulation in bone marrow-derived macrophages by acyltransferases.** *J Biol Chem* 1981, **256**:3690-3697.
48. Hailman E, Lichenstein HS, Wurfel MM, Miller DS, Johnson DA, Kelley M, Busse LA, Zukowski MM, Wright SD: **Lipopolysaccharide (LPS)-binding protein accelerates the binding of LPS to CD14.** *J Exp Med* 1994, **179**:269-277.
49. Friberger P, Sörskog L, Nilsson K, Knös M: **The use of a quantitative assay in endotoxin testing.** In *Detection of Bacterial Endotoxin with the Limulus Amebocyte Lysate Test* Edited by: Watson SW, Levin J, Novitzky TJ. New York: A. Liss; 1987:149-169.

Publish with **BioMed Central** and every scientist can read your work free of charge

"BioMed Central will be the most significant development for disseminating the results of biomedical research in our lifetime."

Sir Paul Nurse, Cancer Research UK

Your research papers will be:

- available free of charge to the entire biomedical community
- peer reviewed and published immediately upon acceptance
- cited in PubMed and archived on PubMed Central
- yours — you keep the copyright

Submit your manuscript here:  
[http://www.biomedcentral.com/info/publishing\\_adv.asp](http://www.biomedcentral.com/info/publishing_adv.asp)

